A Comparison of KNMI Quality Control and JPL Rain Flag for SeaWinds[1]

M. Portabella, A. Stoffelen

KNMI, Postbus 201, 3730 AE De Bilt, The Netherlands

Phone: +31 30 2206827, Fax: +31 30 2210843

e-mail: portabel@knmi.nl, stoffelen@knmi.nl

Abstract

In the past few years, scatterometer winds have been successfully assimilated in weather analysis. A good assessment of the information content of these winds is particularly important for such activities. Besides retrieval problems in cases of a confused sea state, a particularly acute problem of Ku-band scatterometry is the sensitivity to rain. Elimination of poor quality data is therefore a prerequisite for the successful use of the new National Aeronautics and Space Administration (NASA) scatterometer, QuikSCAT. This issue has been the topic of recent work. On the one

[1] Manuscript reference: Portabella, M., and Stoffelen, A., "A Comparison of KNMI Quality Control and JPL Rain Flag for SeaWinds," *Can. Jour. of Rem. Sens.* (special issue on Remote Sensing of Marine Winds), Vol. 28, No. 3, 2002, © Canadian Meteorological Society.

hand, the Royal Dutch Meteorological Institute (KNMI) has developed a quality control (QC) procedure, which detects and rejects the poor quality QuikSCAT data (including rain contamination). On the other hand, the Jet Propulsion Laboratory (JPL) has developed a rain flag for QuikSCAT.

In this paper, we test the KNMI QC against the JPL rain flag in order to improve QC for QuikSCAT. Collocations with European Centre for Medium-range Forecast (ECMWF) winds and Special Sensor Microwave Imager (SSM/I) rain data are used for validation purposes.

The results show that the KNMI QC is more efficient in rejecting low-quality data than the JPL rain fag, while the latter is more efficient in rejecting rain-contaminated data than the former. The JPL rain flag, however, rejects too many consistent wind data in dynamically active areas. The KNMI QC turns out to be a good QC procedure in the parts of the swath where the wind retrieval skill is high. In the nadir region, however, the KNMI QC efficiency and the wind retrieval skill are relatively low. In the nadir region, the KNMI QC needs additional information from the JPL rain flag to reject rain-contaminated data.

1 Introduction

The forecast of extreme weather events is not always satisfactory, while their consequences can have large human and economic impact. The lack of observations over the oceans, where many weather disturbances develop, is one of the main

problems of Numerical Weather Prediction (NWP) for predicting the intensity and position of such disturbances. A space-borne scatterometer with extended coverage is able to provide accurate wind data over the ocean surface and can potentially contribute to improve the situation for tropical and extratropical cyclone prediction [*Isaksen and Stoffelen* (2000) and *Stoffelen and Van Beukering* (1997)].

The impact of observations on weather forecast often critically depends on the Quality Control (QC) applied. For example, *Rohn et al.* (1998) show a positive impact of cloud motion winds on the European Centre for Medium-Range Weather Forecasts (ECMWF) model after QC, while the impact is negative without QC. The effect of QC is also true for scatterometer data. Besides its importance for NWP, in applications such as nowcasting and short-range forecasting, the confidence of meteorologists in the scatterometer data is boosted by a better QC. Therefore, in order to successfully use scatterometer data in any of the mentioned applications, a comprehensive QC needs to be done in advance.

Portabella and Stoffelen (2001) present a QC method (KNMI QC) for SeaWinds scatterometer, based on previous QC work performed by *Stoffelen and Anderson* (1997) and *Figa and Stoffelen* (2000) for the Earth Remote-sensing Satellite (ERS) and NASA (NSCAT) scatterometers, respectively. The KNMI QC is effective in detecting and rejecting Wind Vector Cells (WVC) with poor quality wind information, including rain-contaminated WVCs.

Rain is known to both attenuate and backscatter the microwave signal. *Van de Hulst* (1957) explains these effects. Rain drops are small compared to radar wavelengths and cause Rayleigh scattering (inversely proportional to the fourth power of the wavelength). Large drops are relatively more important in the scattering, and smaller

wavelengths more sensitive. In addition to these effects, there is a "splashing" effect. The roughness of the sea surface is increased because of splashing due to rain drops. This increases the radar backscatter (σ^o) measured, which in turn will affect the quality of wind speed (positive bias due to σ^o increase) and direction (loss of anisotropy in the backscatter signal) retrievals. *Boukabara et al.* (2000) show the variation of the signal measured by a satellite microwave radiometer with the rain rate. As the rain rate increases, the spaceborne instrument sees less and less of the radiation emitted by the surface, and increasingly sees the radiation emitted by the rainy layer that becomes optically thick due to volumetric Rayleigh scattering.

In the presence of extreme weather events, the likelihood of rain is relatively high and QC of SeaWinds particularly important, according to the KNMI experience with near-real time (NRT) processing of SeaWinds data (http://www.knmi.nl/scatterometer). Although the KNMI QC is effective in rejecting rain-contaminated data, additional information on rain may be needed. In this respect, since May 2000, the SeaWinds data products, including the NRT data distributed by the National Oceanic and Atmospheric Administration (NOAA), have a rain flag (*JPL*, 2001). Since both the KNMI QC and the JPL rain flag are used in NRT processing, it is useful to compare them in order to improve the quality control for SeaWinds. For reference, SSM/I is used for rain classification and ECMWF is used for wind validation. For discussion on other rain detection methods, see *Portabella and Stoffelen* (2001).

In section 2, the SeaWinds instrument and the data are presented. In section 3, we briefly describe the KNMI QC and the JPL rain flag. Then, both procedures are compared and validated in section 4. Finally, the summary and recommendations are presented in section 5.

2 Instrument and Data

The SeaWinds instrument onboard the QuikSCAT satellite (launched in June 19, 1999) is a conical-scanning pencil-beam scatterometer. It uses a rotating 1-meter dish antenna with two spot beams, a horizontally-polarized (H-pol) beam and a vertically-polarized (V-pol) beam at incidence angles of 46º and 54º respectively, that sweep in a circular pattern. The antenna radiates microwave pulses at a frequency of 13.4 GHz (Ku-Band) across a 1800-km-wide swath centered on the spacecraft's nadir subtrack, making approximately 1.1 million 25-km ocean surface wind vector measurements and covering 90% of the Earth's surface every day.

The SeaWinds swath is divided into equidistant across-track WVCs or nodes numbered from left to right when looking along the satellite's propagation direction. The nominal WVC size is 25 km x 25 km, and all backscatter measurements centered in a WVC are used to derive the WVC wind solutions. Due to the conical scanning, a WVC is generally viewed when looking forward (fore) and a second time when looking aft. As such, up to four measurement classes emerge: H-pol fore, H-pol aft, V-pol fore, and V-pol aft, in each WVC. Due to the smaller swath (1400 km) viewed in H-pol at 46º degrees incidence, the outer swath WVCs have only V-pol fore and aft backscatter measurements. For more detailed information on the QuikSCAT instrument and data we refer to [*Spencer et al* (1997), *JPL* (2001), *Leidner et al* (2000)].

In order to compare the KNMI QC with the JPL rain flag, we collocate a set of two weeks of QuikSCAT Hierarchical Data Format (HDF) data with ECMWF winds and Special Sensor Microwave Imager (SSM/I) rain data. The HDF data correspond to the reprocessed science data product (version 2.0) produced by JPL using the QSCAT-1 Geophysical Model Function (GMF). The SSM/I instruments are on board Defense Meteorological Satellite Program (DMSP) satellites. We have used DMSP F-13 and F-14 satellites. The collocations with both ECMWF and SSM/I are global. For SSM/I, most of the collocations with the satellite F-13 were found at low latitudes (Tropics), while collocations with F-14 were found at mid and high latitudes. However, the SSM/I collocations which correspond to significant rain were mostly found in the Tropics. In total, there are about 5.2 million collocations with ECMWF and 1.1 million collocations with SSM/I.

The collocations were performed in the following way. For ECMWF, we used the analyses, and 3-hour forecast winds on a 62.5-km grid, and interpolated them both spatially and temporally to the QuikSCAT data acquisition location and time, respectively. For SSM/I, we used the closest SSM/I measurement to the QuikSCAT measurement within the following ranges: 30 minutes time and 0.25º spatial distance.

3 KNMI QC and JPL rain flag descriptions

In this section, we briefly present the KNMI QC and the JPL rain flag pocedures. For more detailed information on the former we refer to *Portabella and Stoffelen* (2001) and on the latter we refer to *Huddleston and Stiles* (2000) and *Mears et al.* (2000).

3.1 KNMI Quality control

The KNMI QC is based on the residual or Maximum Likelihood Estimator (MLE). The MLE indicates how well the backscatter measurements used in the retrieval of a particular wind vector fit the GMF, which is derived for fair weather wind conditions. A large inconsistency with the GMF results in a large MLE, which indicates geophysical conditions other than those modeled by the GMF, such as for example rain, confused sea state, or ice, and as such the MLE provides a good indication for the quality of the retrieved winds.

The method, as described by *Portabella and Stofelen* (2001), consists of normalizing the MLE with respect to the wind and the node number (or cross-track location). The MLE is defined as (adopted from JPL, 2001) :

$$MLE = \frac{1}{N}\sum_{i=1}^{N}\frac{\left(\sigma_{mi}^{o}-\sigma_{s}^{o}\right)^{2}}{kp\left(\sigma_{s}^{o}\right)}, \qquad (1)$$

where N is the number of measurements, σ_{mi}^{o} is the backscatter measurement, σ_{s}^{o} is the backscatter simulated through the GMF for different wind speed and direction trial values, and $kp(\sigma_{s}^{o})$ is the measurement error variance.

Stoffelen and Anderson (1997) interpret the MLE as a measure of the distance between a set of σ_{mi}^{o} values and the solution set σ_{s}^{o} lying on the GMF surface in a transformed measurement space where each axis of the measurement space is scaled by $kp(\sigma_{s}^{o})$.

For a given wind and node number, we compute the expected MLE. Then we define the normalized residual as:

$$Rn = MLE / \langle MLE \rangle \qquad (2)$$

where MLE is the maximum likelihood estimator of a particular wind solution (given by the inversion) and <MLE> is the expected MLE for that particular WVC (node number) and wind solution. The <MLE> is a surface fit to a mean MLE surface which results from computing more than 2 weeks of QuikSCAT data.

Following the definition of Rn, an Rn threshold, which separates the good quality winds from the poor quality winds, needs to be defined. Collocations with ECMWF winds and SSM/I rain data are used in order to tune the Rn threshold in terms of maximum good quality data acceptance and minimum poor-quality data rejection. The Rn threshold is wind dependent. It is a parabolic threshold with a maximum Rn value of 4 at 5 m/s, which reaches a value of 2 at 15 m/s and then remains constant for higher wind speed values. The reference wind speed is the JPL-selected wind solution.

Portabella and Stoffelen (2001) found that the QC procedure works slightly better when using the MLE information of the selected solution rather than the 1st rank solution. Therefore, the Rn is computed with the MLE of the JPL-selected solution (given in the QuikSCAT HDF data product).

The QC by Rn works as follows. The Rn (equation 2) of the JPL-selected solution of any WVC is computed. If the Rn is lower or equal to the threshold, the WVC is accepted; otherwise, the WVC is rejected.

Since May 2000, JPL wind retrievals have been produced using a new GMF called QSCAT-1. In order to perform a consistent comparison with the JPL rain flag (set simultaneouly to QSCAT-1 GMF), the new data should be used. QSCAT-1 is the first empirically derived GMF from QuikSCAT measurements, since the GMF used up to now, NSCAT-2, was derived from NSCAT data. If we invert winds using a different GMF, we will get different MLE values. Although these differences are not expected to be significant, it may well be that Quality Control is affected.

Assuming no major changes, we first compute the Rn using the new QSCAT-1 GMF MLE data and the existing <MLE> surface (computed from NSCAT-2 GMF data). We use collocations with ECMWF and SSM/I to characterize the Rn. The behavior of the Rn as a QC parameter is very similar (not shown) to the behavior of the Rn computed with the NSCAT-2 GMF data by *Portabella and Stoffelen* (2001). Therefore, there is no need to re-compute the <MLE> surface or set a new Rn threshold for the new data; the same QC procedure can be used. Moreover, the QC procedure has been tested for the new data, and indeed the results are very similar to those of *Portabella and Stoffelen* (2001) in terms of maximum good-quality data acceptance and poor-quality data (including rain contamination) rejection,.

3.2 JPL Rain Flag

In January 2000, JPL incorporated in the QuikSCAT products two different rain flags based the mp_rain_probability and the nof_rain_index respectively. However, since May 2000, JPL merged both techniques into a single rain flag. This rain flag procedure is actually based on the mp_rain_probability and called the MUDH (Multidimensional Histogram) rain algorithm (*Huddleston and Stiles, 2000*). The nof_rain_index (*Mears et al., 2000*) is incorporated as an additional parameter in the MUDH rain algorithm, but it is currently not being used (zero weight is assigned to this parameter) in the computation of the rain flag (*JPL, 2001*).

Briefly, mp_rain_probability is the probability of encountering a columnar rain rate that is greater than 2km*mm/hr. This probability value is read directly from a table based on several input parameters including average brightness temperature (both H-pol and V-pol), normalized beam difference, wind speed, wind direction relative to along track, and a normalized MLE. The space spanned by these parameters can detect whether the set of σ^o values used in wind retrieval contain a noteworthy component created by some physical phenomenon other than wind over the ocean's surface, assuming that the most likely phenomenon is rain.

The final rain flag deduced from the MUDH rain algorithm is also incorporated in the QuikSCAT products and can be found in the wvc_quality_flag variable.

4 KNMI QC versus JPL rain flag

The JPL rain flag separates “rain” (rain rate above 2mm/hr) from “no rain” (rain rate below 2 mm/hr) cases and the KNMI QC separates cases of poor-quality to be rejected (above Rn threshold) from those of good quality to be accepted (below Rn threshold).

Both the JPL rain flag and the KNMI QC are meant to separate the usable data from the non-usable data. Therefore, the user should use only “no rain” data according to JPL rain flag and reject the “rain” data. In the same way, the user should accept or reject data according to KNMI QC, and therefore a study of the difference in behaviour of both procedures is of interest.

In order to make a consistent comparison we have processed the HDF data and classified the results in four different categories: A) “JPL Rain Flag - No Rain” and “KNMI QC - Accepted”; B) “JPL Rain Flag - Rain” and “KNMI QC - Accepted”; C) “JPL Rain Flag - No Rain” and “KNMI QC - Rejected”; and D) “JPL Rain Flag - Rain” and “KNMI QC - Rejected”. In line with the previous paragraph, categories A and D show similarities and categories B and C show discrepancies between the two procedures.

4.1 Validation

In tables 1-3, we present the results of collocating the 2 weeks of QuikSCAT HDF data with ECMWF winds and SSM/I rain data. The QuikSCAT data used are from the so-called sweet parts of the swath (WVC numbers 12 to 28 and 49 to 65), i.e. areas with high wind retrieval skill. [Note: we have performed the same validation in the nadir swath (WVC numbers 29 to 48) and got similar results]. We refer to rain data when SSM/I surface rain rate (RR) value is above 2 mm/hr, and to rain-free data when SSM/I surface rain rate value is below 2 mm/hr.

Table 1 shows by category the percentage of total data, the QuikSCAT mean speed, the ECMWF mean speed, the mean bias (QuikSCAT minus ECMWF wind speeds), the mean vector root mean square (RMS) difference between QuikSCAT and ECMWF winds, the percentage of data with rain (RR>2 mm/hr), and the percentage of all rain points (RR>2 mm/hr).

Results in table 1 show a very good agreement between both procedures as 94% of the data corresponds to categories A and D (91.1% in A and 2.9% in D). Moreover, category A shows good quality (0.5 m/s bias and 2.2 m/s RMS) rain-free (only 0.1% of data are rain contaminated) data while category D shows very poor quality (5.1 m/s bias and 8.2 m/s RMS) and rain-contaminated (31.9% of data are rain contaminated) data.

Categories B and C contain 6% of the data and correspond to the differences in behaviour of both procedures.

Comparing both categories in terms of SSM/I rain detection, category B contains 13.9% of all the rain data while category C contains only 2.4%. Therefore, the JPL rain flag is more efficient as rain detector since only 7.6% (5.2% in A and 2.4% in C) of all rain data is not rejected, while the KNMI QC is accepting 19.1% (5.2% in A and 13.9% in B) of rain data.

In terms of quality of the data, both categories contain data of poor quality, with similar bias (2.4 m/s in B and 1.7 m/s in C) and RMS (4.8 m/s in B and 4.1 m/s in C) values. The KNMI QC is more efficient in rejecting poor-quality data than the JPL rain flag since category C contains twice as much data as category B (4% in C; 2% in B). However, the JPL rain flag seems to work reasonably well as a Quality Control flag as categories B and D show that only 27% of that data (13.6% in B and 31.9% in D) are rain contaminated data and therefore the rest are rain-free but still poor-quality data.

Tables 2 and 3 are similar to table 1 but only for rain-free data and rain data respectively. Table 2 contains about 1.1 million data and table 3 about 17000 data.

Table 2 shows very similar results to table 1. The most significant result is that for rain-free data, categories B and D contain poor-quality data, as seen from the high bias (2.2 m/s in B and 4.4 m/s in D) and RMS (4.4 m/s in B and 7 m/s in D). This confirms the JPL rain flag as a Quality Control flag as well.

Table 3 shows the effect of rain in the quality of the data. All categories have larger bias and RMS values compared to tables 1 and 2. In particular, category A contains 5.2% of rainy data, which are clearly of poor quality (2.4 m/s bias and 5.5 m/s RMS). These data are not detected by the JPL rain flag nor the KNMI QC.

The results clearly show that category B contains poor-quality data, including a significant amount of rainy data. Therefore, it seems a good idea to incorporate the JPL rain flag to the KNMI QC in order to improve the Quality Control of QuikSCAT data. However, according to the results in tables 1-3, ECMWF wind speeds in category B are in general significantly higher (up to 4.7 m/s higher) than those in the other categories. This means that category B corresponds to dynamically active situations. Therefore, it could well be that this category systematically corresponds to frontal or low-pressure system areas where the discrepancy between ECMWF and QuikSCAT is indeed of valuable interest and therefore we want this data to be kept and not rejected.

4.2 Meteorological cases

In order to determine the convenience of incorporating the JPL rain flag in the KNMI QC, many meteorological cases were examined. Indeed, some systematic effects were found that help in understanding the statistical results of section 4.1. In this section, we show two wind field examples which are representative of the entire set of examined cases. Figures 1 and 2 show QuikSCAT winds where both the KNMI QC and the JPL rain flag have been applied. The arrows in Figures 1a and 2a correspond to the QuikSCAT JPL-selected wind solutions and the colors represent categories A (green), B (yellow), C (blue) and D (red). Figures 1b and 2b are the same as Figures 1a and 2a, but the arrows corresponding to categories C and D are substituted by dots.

In Figure 1, the presence of a low-pressure system in the western North-Atlantic ocean is clearly discernible in the mid-right part of the plot. A wind front is partly visible going from northeast to south of the low. The KNMI QC has rejected data in the vicinity of the low and along the front line where a confused sea state is expected (see red and blue arrows). We can also see KNMI QC rejections at low-wind areas (blue arrows at bottom part of the plot), where the QuikSCAT retrieved wind flow is clearly inconsistent. As anticipated in the previous section, category-B winds (yellow arrows) are mainly focused in the most dynamical area.

Looking at the same case but only showing category-A and -B winds (accepted winds after KNMI QC), we see that most of the yellow arrows show a spatially consistent flow which we would like to keep. Moreover, the closest Meteosat image (not shown) to the QuikSCAT pass reveals no clouds (therefore no rain) south of the low (where most yellow arrows are located). We discern very few undesirable yellow arrows in the vicinity of the low (most likely poor-quality winds). Therefore, since the consistent category-B winds (yellow) are located in the sweet part of the QuikSCAT swath, it seems that the KNMI QC works fine in these regions.

Figure 2 shows a front line in the middle of the plot associated to a low-pressure system, which is not observed by QuikSCAT, presumably located around 49° North and 314° East. The red arrows in the centre of Figure 2a clearly show the presence of rain bands along the front line. This is confirmed by SSM/I, which detects significant rain (rain rates above 6 mm/hr) in this area. As in the previous case, there is a large number of consistent winds rejected by the JPL rain flag (yellow arrows) in the sweet region (left side of the long black solid lines). Some of these winds are rain-contaminated but the rain rate, according to SSM/I, is around 2 mm/hr. *Portabella*

and Stoffelen (2001) show no significant effect on the quality of high winds at these rain rates.

Looking at the same case but only for the accepted data after KNMI QC (Figure 2b), we still see some inconsistent wind (yellow arrows), which are most likely rain contaminated (unfortunately no SSM/I observations available but Meteosat shows thick clouds over that area) and therefore undesirable. These arrows are located in the nadir region of the swath (between the black solid lines), where KNMI QC is expected to perform less well than in the sweet regions.

Portabella and Stoffelen (2001) report that the reason for the presence of inconsistent wind data lies in the nature of the QC. The QC is based on MLE and therefore on the quality of inversion. In contrast with the sweet regions, in the nadir region there is poor azimuth diversity among observations, which in turn leads to a decrease in the quality of inversion. Subsequently, not only the KNMI QC but also the wind retrieval skills are lower in the nadir region than in the sweet regions of the swath (*Portabella and Stoffelen*, 2001). The lower quality of the retrievals is indicated in the right middle top part of Figure 2b, where several inconsistent winds, which are accepted by both KNMI QC and JPL rain flag (green arrows), are discernible.

From the meteorological cases examined, we can conclude that category B winds are primarily located in dynamically active areas and in many cases they show very consistent wind flows, notably in the sweet swath. However, there are also several rain-contaminated cases and poor-quality winds in the nadir region, which belong to category B (and therefore not detected by KNMI QC) and are undesirable.

Figures 1b and 2b clearly show that rejecting category B winds can significantly reduce the synoptic-scale information content in some meteorological situations.

Nevertheless, in the areas where the beam azimuth diversity is poor and therefore the quality of both the retrievals and the KNMI QC is lower, the rejection of category B winds is necessary.

Therefore, for QuikSCAT QC purposes, we recommend the use of the KNMI QC in the sweet parts of the swath. In the nadir regions however, the combined use of the JPL rain flag and the KNMI QC procedure is recommended.

5 Conclusions

In this paper, a comprehensive comparison of the KNMI QC and the JPL rain flag is performed in order to determine an improved QC procedure for QuikSCAT.

The KNMI QC procedure derived for the NSCAT-2 GMF (*Portabella and Stoffelen, 2001*) is tested with the new GMF (QSCAT-1). Collocations with ECMWF winds and SSM/I rain data are performed for this purpose. The behavior of the Rn computed with the QSCAT-1 GMF MLE is very similar to the behavior of the Rn computed by NSCAT-2 GMF MLE. Therefore the same QC procedure (i.e. same <MLE> surface and Rn threshold) is used for the new QuikSCAT data produced with the QSCAT-1 GMF.

The JPL rain flag is tested against the KNMI QC. Again, the set of collocations with ECMWF winds and SSM/I rain data is used for this comparison. The KNMI QC detects 4% of poor-quality and almost rain-free data, which are not detected by the JPL rain flag. On the other hand, the JPL rain flag detects 2% of poor-quality and

partially rain-contaminated data, which are not detected by the KNMI QC. The KNMI QC is more effective as QC indicator and the JPL rain flag is more effective as a rain detector.

The KNMI QC is based on the MLE parameter, which turns out to be a very good quality control parameter. The JPL rain flag is based not only on the MLE but also on other parameters, which are identified to be sensitive to rain, such as the brightness temperature, the inter-beam difference, the wind direction and others. However, these parameters are not related to the quality of the data, which explains why the KNMI QC works better as quality indicator.

The results also show that the JPL rain flag tends to reject many data in rain-free dynamically active areas. We have illustrated this by two different meteorological cases. In both cases, there is an excess of consistent wind rejections by the JPL rain flag, especially in the sweet parts of the swath. In the nadir region, the wind retrieval skill and consequently the KNMI QC efficiency are lower than in the sweet regions due to the poor beam azimuth diversity. In this area the JPL rain flag is able to detect some flow-inconsistent and rain-contaminated winds which are not detected by KNMI QC.

For the QC of QuikSCAT data, we recommend the use of the KNMI QC. The combination of the JPL rain flag and the KNMI QC is recommended in the nadir region but in the sweet swath the KNMI QC suffices.

As seen in section 4, the wind retrieval skill decreases in the nadir region of the swath in comparison with the sweet swath. We plan to work on the inversion problem in the nadir region to improve the current wind retrieval and consequently the KNMI QC skills.

Acknowledgements

As a member of the KNMI QuikSCAT team, John de Vries has contributed to the work described in this paper. We acknowledge the help and collaboration of our colleagues working at ECMWF and KNMI. The QuikSCAT data were obtained from the NASA Physical Oceanography Distributed Active Archive Center, at the Jet Propulsion Laboratory / California Institute of Technology, and the National Oceanic and Atmospheric Administration. Furthermore, this work was only possible due to the European Meteorological Satellite Organization (EUMETSAT) grant for a research fellowship post at KNMI.

References

Boukabara, S.A., Hoffman, R.N., and Grassotti, C., "Atmospheric Compensation and Heavy Rain Detection for SeaWinds Using AMSR," *Atmospheric Environmental Research Inc.*, 131 Hartwell Ave., Lexington, Massachussets (USA), 2000.

Figa, J., and Stoffelen, A., "On the Assimilation of Ku-band Scatterometer Winds for Weather Analysis and Forecasting," *IEEE Trans. on Geoscience and Rem. Sens.* 38 (4) pp. 1893-1902, 2000.

Huddleston, J.N., and Stiles, B.W., "A Multi-dimensional Histogram Technique for Flagging Rain Contamination on QuikSCAT," *Proc. of IEEE International Geoscience and Remote Sensing Symposium*, Vol. 3, Honolulu (USA), IEEE, pp. 1232-1234, 2000.

Isaksen, L., and Stoffelen, A., "ERS Scatterometer Wind Data Impact on ECMWF's Tropical Cyclone Forecasts," *IEEE Trans. on Geoscience and Rem. Sens.* 38 (4) pp. 1885-1892, 2000.

JPL, "QuikSCAT Science Data Product User's Manual," version 2.2, *JPL* D-18053, pp. 89, 2001.

Leidner, M., Hoffman, R., and Augenbaum, J., "SeaWinds Scatterometer Real-Time BUFR Geophysical Data Product," version 2.2.0, *NOAA/NESDIS*, pp. 45, 2000.

Mears, C., Smith, D., and Wentz F., "Detecting Rain with QuikSCAT," *Proc. of International Geoscience and Remote Sensing Symposium*, Vol. 3, Honolulu (USA), IEEE, pp. 1235-1237, 2000.

Portabella, M., and Stoffelen, A., "Rain Detection and Quality Control of SeaWinds," *J. Atm. And Ocean Techn*., Vol. 18, No. 7, pp. 1171-1183, 2001.

Rohn, M., Kelly, G., and Saunders, R., "Experiments with Atmospheric Motion Vectors at ECMWF," *Proc. of Fourth International Winds Workshop*, EUM P24, ISSN 1023-0416, Saanenmoser (Switzerland), EUMETSAT, pp. 139-146, 1998.

Spencer, M.W., Wu, C., and Long, D.G., "Tradeoffs in the Design of a Spaceborn Scanning Pencil Beam Scatterometer: Apllication to SeaWinds," *IEEE Trans. Geosci. Remote Sensing*, Vol. 35, No. 1, pp. 115-126, 1997.

Stoffelen, A., and Anderson D., "Scatterometer Data Interpretation: Measurement Space and Inversion," *J. Atm. And Ocean Techn*., 14(6), pp. 1298-1313, 1997.

Stoffelen, A., Van Beukering, P., "Implementation of Improved ERS Scatterometer Data Processing and its Impact on HIRLAM Short Range Weather Forecasts," *Beleidscomissie Remote Sensing Report*, contract NRSP-2/97-06, pp. 75, 1997.

Van De Hulst, H.C., "Light Scattering by small particles," *John Wiley and Sons*, New York, pp. 428, 1957.

Figure legends

Figure 1 QuikSCAT wind fields. The colors represent the different categories: green is category A, yellow is B, purple is C, and red is D. Plot a shows all retrieved winds while plot b shows only KNMI QC accepted winds. The black solid lines separate different regions of the swath. In this case, the left side of the plot corresponds to the sweet-right region, the middle to the nadir region and the right side to the sweet-left region. The acquisition date is February 14 2001 at 22 hours UTC.

Figure 2 Same as Figure 1 but for different date (January 20 2001 at 20:30 hours UTC) and location. As in the previous figure, the black solid lines separate the sweet-right (left side), the nadir (middle) and the sweet-left (right side) regions QuikSCAT wind fields

Tables

Table 1. Comparison for all data

	JPL Rain Flag No Rain	JPL Rain Flag Rain
KNMI QC Accepted	Number of data (%): 91.1 QuikSCAT Mean Speed (m/s): 7.6 ECMWF Mean Speed (m/s): 7.1 Mean Bias (m/s): 0.5 Mean RMS (m/s): 2.2 Rain > 2 mm/hr (%[1]): 0.1 Rain > 2 mm/hr (%[2]): 5.2	Number of data (%): 2.0 QuikSCAT Mean Speed (m/s): 14.2 ECMWF Mean Speed (m/s): 11.8 Mean Bias (m/s): 2.4 Mean RMS (m/s): 4.8 Rain > 2 mm/hr (%[1]): 13.6 Rain > 2 mm/hr (%[2]): 13.9
KNMI QC Rejected	Number of data (%): 4.0 QuikSCAT Mean Speed (m/s): 9.1 ECMWF Mean Speed (m/s): 7.4 Mean Bias (m/s): 1.7 Mean RMS (m/s): 4.1 Rain > 2 mm/hr (%[1]): 1.0 Rain > 2 mm/hr (%[2]): 2.4	Number of data (%): 2.9 QuikSCAT Mean Speed (m/s): 12.3 ECMWF Mean Speed (m/s): 7.2 Mean Bias (m/s): 5.1 Mean RMS (m/s): 8.2 Rain > 2 mm/hr (%[1]): 31.9 Rain > 2 mm/hr (%[2]): 78.5

[1] : % of data in this category with rain (RR> 2 mm/hr)

[2] : % of all rain points (RR>2mm/hr)

Table 2. Comparison for rain-free data

	JPL Rain Flag No Rain	JPL Rain Flag Rain
KNMI QC Accepted	A Number of data (%): 92.7 QuikSCAT Mean Speed (m/s): 7.0 ECMWF Mean Speed (m/s): 6.5 Mean Bias (m/s): 0.5 Mean RMS (m/s): 2.0	B Number of data (%): 1.3 QuikSCAT Mean Speed (m/s): 12.2 ECMWF Mean Speed (m/s): 10.0 Mean Bias (m/s): 2.2 Mean RMS (m/s): 4.4
KNMI QC Rejected	C Number of data (%): 3.5 QuikSCAT Mean Speed (m/s): 7.8 ECMWF Mean Speed (m/s): 5.9 Mean Bias (m/s): 1.9 Mean RMS (m/s): 4.2	D Number of data (%): 2.5 QuikSCAT Mean Speed (m/s): 10.3 ECMWF Mean Speed (m/s): 5.9 Mean Bias (m/s): 4.4 Mean RMS (m/s): 7.0

Table 3. Comparison for rain data

	JPL Rain Flag No Rain	JPL Rain Flag Rain
KNMI QC Accepted	A Number of data (%): 5.2 QuikSCAT Mean Speed (m/s): 10.8 ECMWF Mean Speed (m/s): 8.4 Mean Bias (m/s): 2.4 Mean RMS (m/s): 5.5	B Number of data (%): 13.9 QuikSCAT Mean Speed (m/s): 13.7 ECMWF Mean Speed (m/s): 9.0 Mean Bias (m/s): 4.7 Mean RMS (m/s): 8.2
KNMI QC Rejected	C Number of data (%): 2.4 QuikSCAT Mean Speed (m/s): 9.9 ECMWF Mean Speed (m/s): 6.6 Mean Bias (m/s): 3.3 Mean RMS (m/s): 6.1	D Number of data (%): 78.5 QuikSCAT Mean Speed (m/s): 14.4 ECMWF Mean Speed (m/s): 6.4 Mean Bias (m/s): 8.0 Mean RMS (m/s): 11.2

Figures

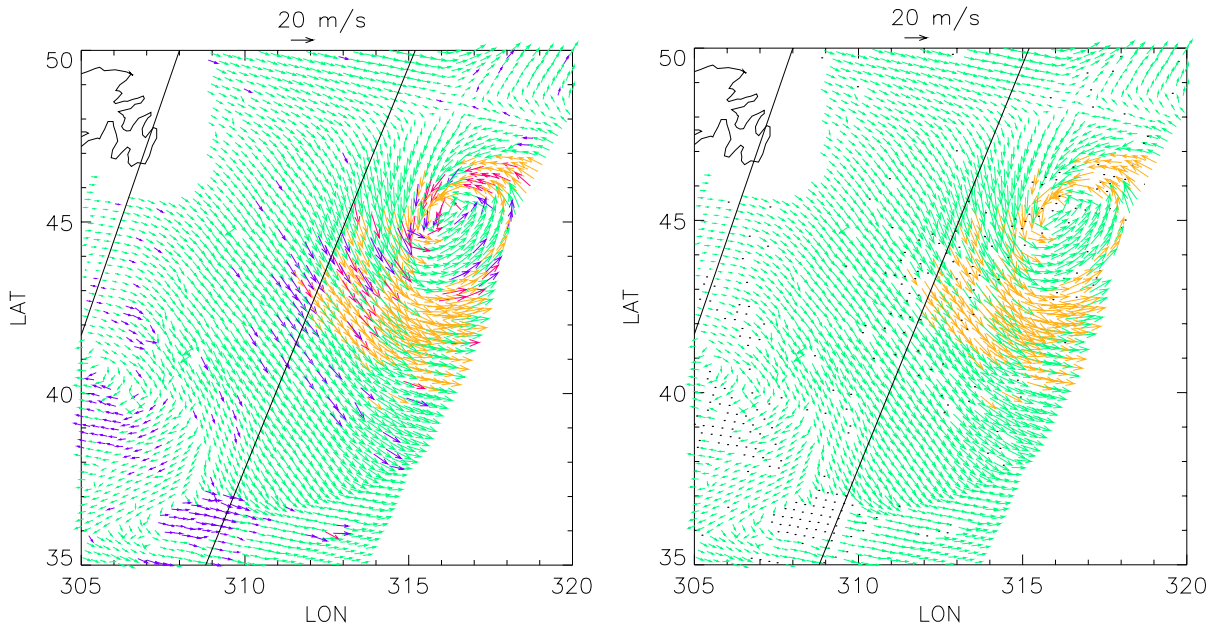

a) b)

Figure 1 QuikSCAT wind fields. The colors represent the different categories: green is category A, yellow is B, purple is C, and red is D. Plot a shows all retrieved winds while plot b shows only KNMI QC accepted winds. The black solid lines separate different regions of the swath. In this case, the left side of the plot corresponds to the sweet-right region, the middle to the nadir region and the right side to the sweet-left region. The acquisition date is February 14 2001 at 22 hours UTC.

CASE : 20/01/01 2030 UTC

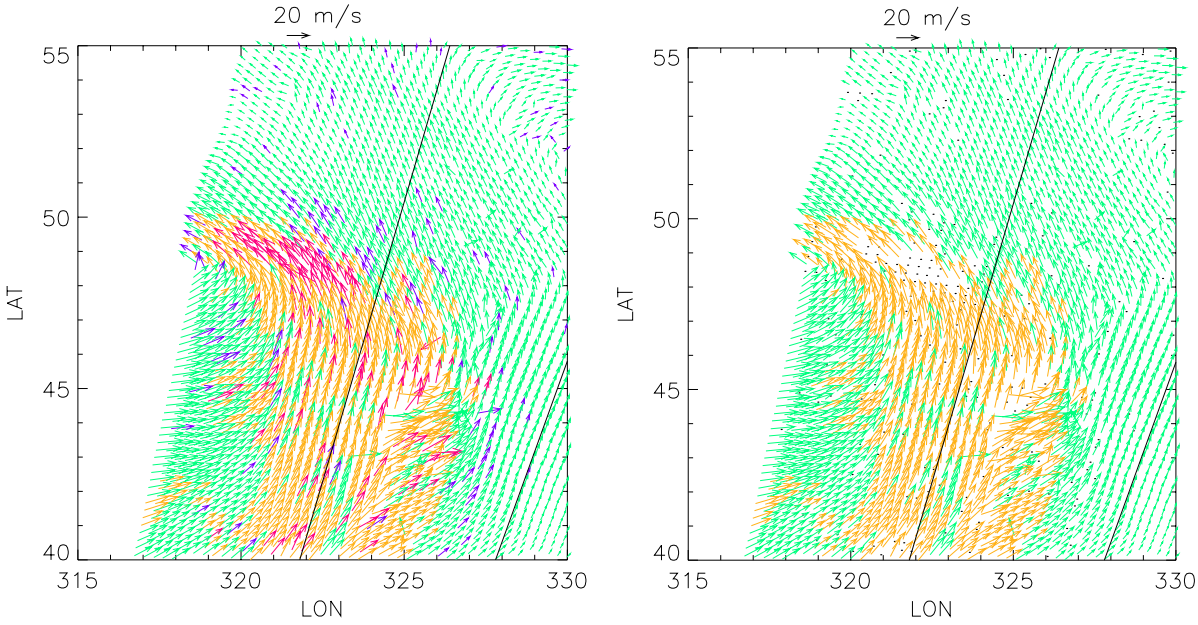

a) b)

Figure 2 Same as Figure 1 but for different date (January 20 2001 at 20:30 hours UTC) and location. As in the previous figure, the black solid lines separate the sweet-right (left side), the nadir (middle) and the sweet-left (right side) regions QuikSCAT wind fields.